

Constructing a variational family for nonlinear state-space models

Jarrad Courts^{*1}, Christopher Renton^{†2}, Thomas B. Schön^{‡3}, and Adrian Wills^{§4}

¹*School of Engineering, University of Newcastle, Australia*

²*School of Engineering, University of Newcastle, Australia*

³*Department of Information Technology, Uppsala University, Sweden*

⁴*School of Engineering, University of Newcastle, Australia*

February 10, 2020

Abstract

We consider the problem of maximum likelihood parameter estimation for nonlinear state-space models. This is an important, but challenging problem. This challenge stems from the intractable multidimensional integrals that must be solved in order to compute, and maximise, the likelihood. Here we present a new variational family where variational inference is used in combination with tractable approximations of these integrals resulting in a deterministic optimisation problem. Our developments also include a novel means for approximating the smoothed state distributions. We demonstrate our construction on several examples and show that they perform well compared to state of the art methods on real data-sets.

1 Introduction

Mathematical models of system dynamics are a core technology in most model-based engineered systems acting and interacting with their environment. Examples include GPS, autonomous vehicles, passenger aircraft and robotics, to name just a few. The remarkable utility of mathematical models stems from the fact that, *inter alia*, they enable decision making based on prediction of system behaviour under new scenarios, accelerate the analysis and design processes, are fundamental to detecting faults or changes, and they are capable of handling *uncertainty* that is present in data, assumptions and algorithms.

Motivated by the broad applicability and utility of modelling, the scientific community has devoted significant research attention towards learning dynamical models from data. Importantly, for dynamic systems, the sequence or ordering of the data must be maintained as future outcomes are deemed to be fundamentally related to the past. This is sometimes called *sequence learning* (Sun and Giles, 2001) or *system identification* (Ljung, 1999). In essence, these approaches search over a space of models and determine the model that best (in some sense) fits the data while maintaining the time ordering.

The current paper is directed towards solving this important problem. To make these ideas more concrete, here we assume that data from the system of interest is available in the form of a data record $y_{1:T} \triangleq \{y_1, \dots, y_T\}$, where each measurement y_k is potentially multidimensional and the number of available measurements is denoted as $T > 0$. We further assume that the data may be adequately described as an instance from a joint distribution that is parametrized by an unknown vector θ (called the *parameter vector*), that is (with abuse of notation)

$$y_{1:T} \sim p_\theta(y_{1:T}). \quad (1)$$

A highly successful approach to learning θ based on $y_{1:T}$ is the so-called Maximum-Likelihood approach (Fisher, 1922), where the parameter vector θ is determined as any maximiser of the log-likelihood $\log p_\theta(y_{1:T})$ (noting that the logarithm function does not affect the maximiser)

$$\hat{\theta}_{\text{ML}} = \arg \max_{\theta} \log p_\theta(y_{1:T}). \quad (2)$$

*Jarrad.Courts@uon.edu.au

†Christopher.Renton@newcastle.edu.au

‡thomas.schon@it.uu.se

§Adrian.Wills@newcastle.edu.au

There are two essential difficulties with this approach. First is the mathematical description of how θ affects $p_\theta(\cdot)$. The choices here are vast (see e.g., [Ljung \(2008\)](#)), but we will employ the flexible class of so-called nonlinear state-space models (to be described below). Secondly, evaluating the likelihood (and possibly its gradient and higher order derivatives) that are often essential to solving (2) may not be computationally tractable ([Kantas et al., 2015](#)).

With regard to the first difficulty, we assume that the dynamic response can be described using a state-space model. Here the output data y_k is related to a *hidden* (or latent) quantity x_k , which is called the state, and the state is assumed to evolve over time. More specifically, the state evolution and data likelihood are assumed to satisfy

$$x_{k+1} | x_k \sim p_\theta(x_{k+1} | x_k), \quad y_k | x_k \sim p_\theta(y_k | x_k). \quad (3)$$

With regard to the second difficulty, the joint log-likelihood $p_\theta(y_{1:T})$ can be expressed as ([Jazwinski, 1970](#))

$$\log p_\theta(y_{1:T}) = \sum_{k=1}^T \log \int p_\theta(y_k | x_k) p_\theta(x_k | y_{1:k-1}) dx_k,$$

where the so-called state prediction distribution $p_\theta(x_k | y_{1:k-1})$ can be expressed via the recursion

$$p_\theta(x_{k+1} | y_{1:k}) = \int \frac{p_\theta(y_k | x_k) p_\theta(x_{k+1} | x_k)}{p_\theta(y_k | y_{1:k-1})} p_\theta(x_k | y_{1:k-1}) dx_k. \quad (4)$$

The difficulty in evaluating the above expressions is that they involve multidimensional integrals, which in general do not have known closed-form solutions. Additionally, classical numerical integration quickly becomes computationally intractable as the state dimension grows. Due to this inherent barrier, researchers have investigated several approximations. Among the most successful are the so-called Sequential Monte-Carlo (SMC) methods ([Gordon et al., 1993](#); [Kitagawa, 1993](#); [Stewart and McCarty, 1992](#)) and variational methods ([Jordan et al., 1999](#)). Work related to these approaches is briefly outlined in Section 5.

In the current paper, we investigate the variational approach [Jordan et al. \(1999\)](#) and form a tractable and deterministic approximation to an exact lower bound of $\log p_\theta(\mathbf{y})$. Broadly speaking, by introducing a *novel* variational distribution family q_β , which is independently parameterised by β , we are free to choose q_β such that tractable, and deterministic, approximations bounding the likelihood are readily available. This approximation is then jointly optimised over all unknown parameters (θ, β) .

Importantly, since the resulting optimisation problem is deterministic, we can rely on off-the-shelf solvers to efficiently solve the problem. An implication of this technique is that it provides a new method of forming smoothed state distributions. This allows for the variational-inference (VI) approach to be linked with the expectation-maximisation (EM) approach [Dempster et al. \(1977\)](#).

The main contributions of this paper are summarised as follows:

1. A new variational distribution tailored to nonlinear state-space models (Section 2).
2. The use of this variational distribution for joint parameter (θ, β) inference from data $y_{1:T}$ (Section 3).
3. The provision of a clear link between variational-inference and EM based parameter estimation approaches (Section 3.2).
4. Extensive numerical experiments on both real and simulated data supporting the efficacy of the new construction (Section 4).

2 Constructing the variational distribution

This section outlines the VI approach, which results in a lower bound of the likelihood (see Section 2.1), and details our proposed distribution class (see Section 2.2).

2.1 VI Approximation

Exploiting conditional probability, we can express the log-likelihood as

$$\log p_\theta(\mathbf{y}) = \log p_\theta(\mathbf{x}, \mathbf{y}) - \log p_\theta(\mathbf{x} | \mathbf{y}), \quad (5)$$

where $\mathbf{x} \triangleq x_{0:T} \triangleq \{x_0, \dots, x_T\}$ is the unobserved state sequence.

Employing the VI principle (Jordan et al., 1999), we introduce the variational distribution $q_\beta(\mathbf{x} | \mathbf{y})$ for the joint state, where $\beta \in \mathbb{R}^{n_\beta}$ is a vector of parameters. By adding and subtracting $\log q_\beta(\mathbf{x} | \mathbf{y})$ to (5), we have

$$\log p_\theta(\mathbf{y}) = \log \frac{p_\theta(\mathbf{x}, \mathbf{y})}{q_\beta(\mathbf{x} | \mathbf{y})} + \log \frac{q_\beta(\mathbf{x} | \mathbf{y})}{p_\theta(\mathbf{x} | \mathbf{y})}, \quad (6)$$

where $q_\beta(\mathbf{x} | \mathbf{y})$ is assumed to have support for $p_\theta(\mathbf{x}, \mathbf{y})$. Furthermore, since $\log p_\theta(\mathbf{y})$ is not a function of \mathbf{x} , then

$$\log p_\theta(\mathbf{y}) = \int \log p_\theta(\mathbf{y}) q_\beta(\mathbf{x} | \mathbf{y}) d\mathbf{x}. \quad (7)$$

Substituting (6) into (7) yields

$$\log p_\theta(\mathbf{y}) = \mathcal{L}(\theta, \beta) + \text{KL}[q_\beta(\mathbf{x} | \mathbf{y}) || p_\theta(\mathbf{x} | \mathbf{y})], \quad (8)$$

where $\mathcal{L}(\theta, \beta)$ is defined as

$$\mathcal{L}(\theta, \beta) = \int \log \frac{p_\theta(\mathbf{x}, \mathbf{y})}{q_\beta(\mathbf{x} | \mathbf{y})} q_\beta(\mathbf{x} | \mathbf{y}) d\mathbf{x}, \quad (9)$$

and $\text{KL}[q(\cdot) || p(\cdot)] \geq 0$ is the Kullback-Leibler divergence from $p(\cdot)$ to $q(\cdot)$. Therefore, $\mathcal{L}(\theta, \beta)$ is a lower bound for $\log p_\theta(\mathbf{y})$. Importantly, the tractability of calculating $\mathcal{L}(\theta, \beta)$ is influenced by the choice of $q_\beta(\mathbf{x} | \mathbf{y})$. Due to the Markovian nature of state-space models, $\mathcal{L}(\theta, \beta)$ can be written as

$$\mathcal{L}(\theta, \beta) = I_1 + I_2 + I_3 - I_4,$$

where

$$\begin{aligned} I_1 &= \int q_\beta(x_0 | \mathbf{y}) \log p(x_0) dx_0, \\ I_2 &= \sum_{k=0}^{T-1} \int q_\beta(x_{k:k+1} | \mathbf{y}) \log p_\theta(x_{k+1} | x_k) dx_{k:k+1}, \\ I_3 &= \sum_{k=1}^T \int q_\beta(x_k | \mathbf{y}) \log p_\theta(y_k | x_k) dx_k, \\ I_4 &= \int q_\beta(\mathbf{x} | \mathbf{y}) \log q_\beta(\mathbf{x} | \mathbf{y}) d\mathbf{x}, \end{aligned}$$

and $p(x_0)$ is a given prior distribution on x_0 . The integral I_4 can be further expanded (Vrettas et al., 2008) into

$$\begin{aligned} I_4 &= \sum_{k=0}^{T-1} \int q_\beta(x_{k:k+1} | \mathbf{y}) \log q_\beta(x_{k:k+1} | \mathbf{y}) dx_{k:k+1} \\ &\quad - \sum_{k=1}^{T-1} \int q_\beta(x_k | \mathbf{y}) \log q_\beta(x_k | \mathbf{y}) dx_k. \end{aligned} \quad (10)$$

It can be seen from $I_{1:4}$ that $\mathcal{L}(\theta, \beta)$ does not require the full parametric distribution, but rather only the marginal and pairwise joint elements are required.

2.2 Proposed Distribution Class

It is now assumed that the parametric distribution is selected to be normally distributed. As such the pairwise joint distributions can be given as

$$q_{\beta_k}(x_{k+1}, x_k) = \mathcal{N} \left(\begin{bmatrix} x_k \\ x_{k+1} \end{bmatrix}; \begin{bmatrix} \mu_k \\ \eta_{k+1} \end{bmatrix}, \begin{bmatrix} P_k & M_k \\ M_k^T & \Sigma_{k+1} \end{bmatrix} \right),$$

subject to the constraints

$$\mu_k = \eta_k, \quad P_k = \Sigma_k, \quad \begin{bmatrix} P_k & M_k \\ M_k^T & \Sigma_{k+1} \end{bmatrix} \succ 0, \quad (11)$$

for all k . The marginal distributions are then of the form

$$q_{\beta_k}(x_k) = \mathcal{N}(x_k; \mu_k, P_k). \quad (12)$$

The parameters $\beta \triangleq \{\beta_0, \dots, \beta_{T-1}\}$ are now given as

$$\beta_k = \{\mu_k, \eta_{k+1}, P_k, M_k, \Sigma_{k+1}\}. \quad (13)$$

We now focus on evaluating each integral within $\mathcal{L}(\theta, \beta)$. Since q_{β} is normal, I_4 is readily evaluated in closed form. Furthermore, if we assume the prior takes the form $p(x_0) = \mathcal{N}(x_0; \mu_p, \Sigma_p)$, then I_1 is similarly evaluated. The remaining terms, I_2 and I_3 , are intractable Gaussian expectations of the form

$$\mathbb{E}[g(x)] = \int \mathcal{N}(x; \mu, P) g(x) dx, \quad (14)$$

where $g(x) : \mathbb{R}^n \rightarrow \mathbb{R}$ is a nonlinear function. Gaussian quadrature approximation,

$$\mathbb{E}[g(x)] \approx \sum_{j=1}^{n_s} w_j g(x^j), \quad (15)$$

with n_s sigma points x^j with corresponding weights w_j determined as functions of μ and P , enables tractable approximations of I_2, I_3 to be obtained, denoted \hat{I}_2, \hat{I}_3 respectively. Thus, we can approximate $\mathcal{L}(\theta, \beta)$ by

$$\hat{\mathcal{L}}(\theta, \beta) = I_1 + \hat{I}_2 + \hat{I}_3 - I_4. \quad (16)$$

3 Using the Construction

Let us now detail how our variational distribution class can be applied to jointly estimate both model parameters and the state distributions. This is performed in both the general case (see Section 3.1.1) and for an important subclass (see Section 3.1.2) that enables additional simplifications. We then link our proposed joint estimation method to the classical EM approach in Section 3.2.

3.1 Joint parameter and state estimation

3.1.1 General Nonlinear State Space models

The proposed approach to the ML parameter estimation problem is to perform optimisation jointly over θ and β ,

$$\theta^*, \beta^* = \arg \max_{\theta, \beta} \hat{\mathcal{L}}(\theta, \beta) \quad \text{s.t.} \quad (31), \quad (17)$$

which is performed using a standard optimisation routine that exploits exact gradient and Hessian information.

To ensure that this optimisation problem remains practical to solve for large T , we introduce independent copies of the parameter vector θ for each timestep, denoted θ_i , where we enforce the constraints $\theta_0 = \theta_1 = \dots = \theta_T$ to maintain equivalence with (17). The vector of optimisation variables is formed by interleaving the vectorisation of β and θ in the following sequence: $\text{vec}(\beta_0), \theta_0, \dots, \text{vec}(\beta_T), \theta_T$. This results in a sparse block-diagonal Hessian, which ensures linear time complexity in the Hessian formation and subsequent step direction solution.

3.1.2 An Important Class of Systems

We consider a model structure of the form

$$x_{k+1} = f(x_k, \phi) + q_k, \quad y_k = h(x_k, \phi) + r_k, \quad (18)$$

where $q_k \sim \mathcal{N}(0, Q)$, $r_k \sim \mathcal{N}(0, R)$, and $\theta = \{\phi, Q, R\}$ includes model parameters, process noise parameters, and measurement noise parameters.

From (15) and (18), we can evaluate \hat{I}_2 and \hat{I}_3 as follows:

$$\hat{I}_2 = -\frac{T}{2} \log |2\pi Q| - \frac{1}{2} \sum_{k=0}^{T-1} \sum_{j=1}^{n_s} w_j \left\| \xi_k^j \right\|_{Q^{-1}}^2, \quad (19a)$$

$$\hat{I}_3 = -\frac{T}{2} \log |2\pi R| - \frac{1}{2} \sum_{k=1}^T \sum_{j=1}^{n_s} w_j \left\| \varepsilon_k^j \right\|_{R^{-1}}^2, \quad (19b)$$

where

$$\xi_k^j = x_{k+1}^j - f(x_k^j, \phi), \quad \varepsilon_k^j = y_k - h(x_k^j, \phi), \quad (20)$$

and (x_k^j, x_{k+1}^j) are sigma points from the joint normal distribution $q_{\beta_k}(x_k, x_{k+1})$.

It is readily verified that the optimum parameters Q^* and R^* satisfy

$$Q^*(\phi, \beta) = \frac{1}{T} \bar{x} \bar{x}^T, \quad R^*(\phi, \beta) = \frac{1}{T} \bar{y} \bar{y}^T, \quad (21)$$

where

$$\begin{aligned} \bar{x} &= [\bar{x}_0, \dots, \bar{x}_{T-1}], & \bar{x}_k &= [\sqrt{w_1} \xi_k^1, \dots, \sqrt{w_{n_s}} \xi_k^{n_s}], \\ \bar{y} &= [\bar{y}_1, \dots, \bar{y}_T], & \bar{y}_k &= [\sqrt{w_1} \varepsilon_k^1, \dots, \sqrt{w_{n_s}} \varepsilon_k^{n_s}]. \end{aligned}$$

Substituting (21) into (19a) and (19b) yields

$$I_2^{\text{ID}} = c_2 - \frac{T}{2} \log |Q^*(\phi, \beta)|, \quad (22a)$$

$$I_3^{\text{ID}} = c_3 - \frac{T}{2} \log |R^*(\phi, \beta)|, \quad (22b)$$

respectively, where c_2 and c_3 are constants. Thus, we can pose the reduced problem,

$$\phi^*, \beta^* = \arg \max_{\phi, \beta} \hat{\mathcal{L}}_{\text{ID}}(\phi, \beta) \quad \text{s.t.} \quad (31). \quad (23)$$

where $\hat{\mathcal{L}}_{\text{ID}}(\phi, \beta) = I_1 + I_2^{\text{ID}} + I_3^{\text{ID}} - I_4$. Estimates of Q and R are obtained by evaluating $Q^*(\phi^*, \beta^*)$ and $R^*(\phi^*, \beta^*)$, respectively.

Details of the numerical implementation of this approach are provided in the supplementary material. This includes the efficient evaluation of the gradient and Hessian by exploiting the available structure.

3.2 Connection to EM

Whilst we have examined joint optimisation of (θ, β) , we could alternatively perform block co-ordinate descent. Indeed by selecting θ and β to be the blocks we arrive at a VI based EM approach (VI EM). Using the notation of Schön et al. (2011) this can be written as

$$\mathcal{Q}(\theta, \theta') = I_1 + I_2 + I_3, \quad (24)$$

noting that I_4 is independent of θ . Our variational construction can hence be utilised within the EM framework if desired by iteratively performing the following steps:

$$\text{(E-step)} : \quad \beta^* = \arg \max_{\beta} \hat{\mathcal{L}}(\theta, \beta),$$

$$\text{(M-step)} : \quad \theta^* = \arg \max_{\theta} \hat{\mathcal{L}}(\theta, \beta^*).$$

Additionally, in the situation where θ is assumed known, the E-step can also be used as a VI-based assumed density smoother. The performance of such a smoother is tested in Section 4. A detailed discussion of this smoothing approach and how it differs from existing methods is found in the supplementary material.

4 Examples

In this section, we present numerical results of our proposed method on several structurally different state space models with both simulated and real data and compare the results with exact linear EM (Gibson and Ninness, 2005), unscented Rauch-Tung-Striebel smoothing Särkkä (2008) based EM (URTSS EM) Gašperin and Juričić (2011) and particle stochastic approximation EM (SAEM) based upon Lindsten (2013). The Variational Sequential Monte Carlo method (Naesseth et al., 2018) was also examined for comparison, but was found to be computationally prohibitive for the examples we have considered and further details are found in the supplementary material.

For our proposed method, the unscented transform is utilised as the Gaussian quadrature scheme and all optimisation is performed using `fmincon` MATLAB (2018) with default tolerances unless otherwise stated. All code and data-sets required to reproduce these results will be made available.

4.1 Linear Scalar Model

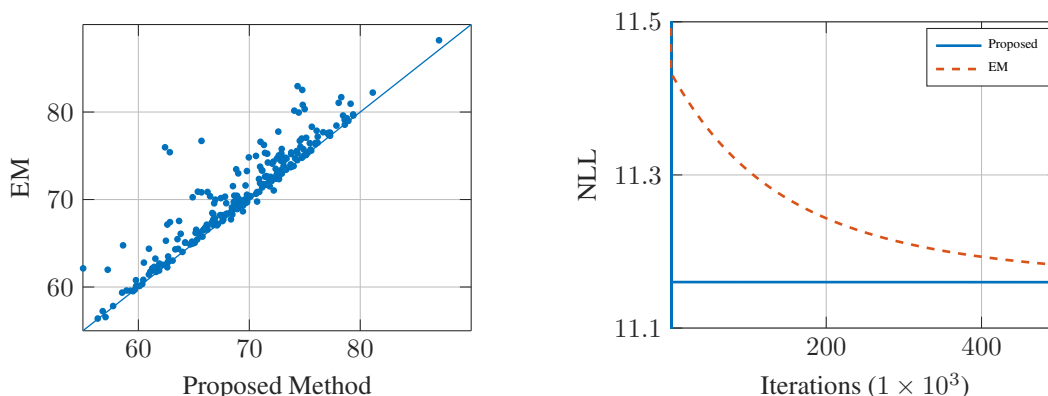
In this example, we consider the identification of the following system using 50 measurements:

$$x_{k+1} = ax_k + bu_k + v_k, \quad y_k = cx_k + du_k + e_k,$$

where $v_k \sim \mathcal{N}(0, q)$, $e_k \sim \mathcal{N}(0, r)$, and the true parameters are given by $\theta = [a, b, c, d, q, r]^T = [0.9, 1, 1, 0, 1, 0.01]^T$, the initial state is 0.1, the prior distribution is $p(x_0) = \mathcal{N}(0.15, 1)$, and the inputs are drawn from a standard normal. The initial parameter estimates used for identification are given by $\theta_0 = [0.9 + w_1, 1 + w_2, 1 + w_3, w_4, 1, 0.01]^T$ where $w_i \sim \mathcal{N}(0, 0.5^2)$. The state distributions used to initialise the proposed method are the smoothed state distribution found using θ_0 .

We first compare 100 iterations of the method proposed in Section 3.1.2 with a sparse Hessian approximation (see supplementary material) against 100 iterations of linear EM. The results of 250 separate runs are shown in Figure 1a, which compares the negative log-likelihood (NLL) obtained with each point above the diagonal reference line indicating the proposed method has outperformed EM for that trial.

To compare the convergence rates of both methods, we use a model defined by $\theta = [0.9, 1, 1, 0, 0.1, 0.1]^T$, and initialised at $\theta_0 = [1.8, 3, 4, 0, 0.6, 0.7]^T$ with a prior of $p(x_0) = \mathcal{N}(0.15, 0.01)$. For this model, our proposed identification method ran until convergence to a local minima, requiring 1635 iterations taking 25.29 s. The EM method ran until the iteration limit of 500 000 and ran for 493.55 s. The results shown in Figure 1b highlight that the slow convergence of EM prevented it matching the performance of our proposed method. The results shown



(a) Comparison of NLL obtained after 100 iterations of EM and the proposed method. Points above the diagonal reference line indicate the proposed method has outperformed exact EM for that trial.

(b) Convergence behaviour of both EM and the proposed method near a solution. The dashed line is the final converged value achieved using the proposed method, which required 1635 iterations.

Figure 1: Comparisons of exact EM and the proposed method both at 100 iterations and at the limit of final convergence.

in Figure 1a demonstrate that our proposed method can deliver effective identification results and can slightly outperform exact linear EM. This appears due to the differing convergence properties our method and EM possess, which can be explained using the co-ordinate descent interpretation of EM in Section 3.2.

4.2 Nonlinear Scalar Model

In this example, we consider 50 timesteps of the following nonlinear system:

$$x_{t+1} = ax_t + b \frac{x_t}{1 + x_t^2} + c \cos(1.2t) + v_t \quad (26a)$$

$$y_t = cx_t^2 + e_t, \quad (26b)$$

where $v_t \sim \mathcal{N}(0, q)$ and $e_t \sim \mathcal{N}(0, r)$.

We first compare the VI smoother from Section 3.2 against the URTSS and a grid-based reference solution for both likelihoods and state distributions (see supplementary). The true parameters are $\theta = [a, b, c, d, q, r]^T = [0.5, 2, 8, 0.05, 1, 0.01]^T$, the initial state is 0.1, and the prior distribution is $p(x_0) = \mathcal{N}(0.15, 1)$. State estimation is performed using $\theta_0 = [0.5, 5, 8, 0.05, 1, 0.01]^T$. To initialise the VI smoother, the state distributions from a VI-based filter are used. This filter consists of iteratively performing VI smoothing over two time steps and marginalising to obtain a filtered distribution. Each of these sub-problems are initialised using the predicted joint distribution.

Figure 2 plots the state distributions for a single time step and shows that the VI smoother has well approximated the true smoothed distribution. In contrast, the URTSS has performed poorly, which may be caused by the assumption made that both the predicted and filtered distributions are Gaussian. Figure 3 shows that the VI smoother

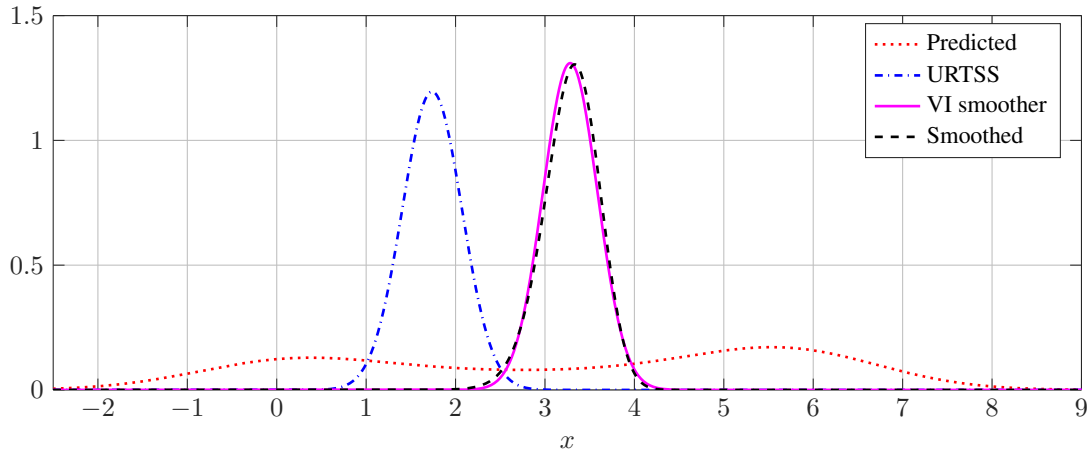


Figure 2: Predicted and smoothed state distributions for a single time step.

consistently had a smaller KL divergence from the true smoothed distribution compared with the URTSS approach across all time steps.

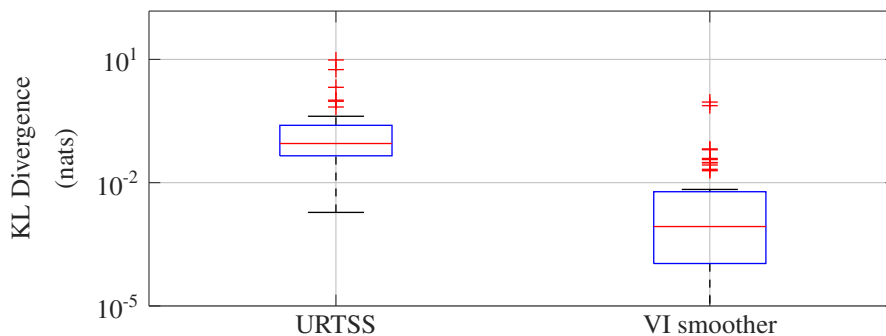


Figure 3: Boxplots of the KL divergence between estimated and true smoothed state distributions for each timestep showing the VI smoother has consistently outperformed the URTSS.

We now examine the robustness of the method proposed in Section 3.1.2 using a dense Hessian approximation to the initial parameter estimates. For this, the true parameters are given by $\theta = [0.5, 2, 8, 0.05, 0, 0.01]^T$ whilst

initial estimates are sampled from $\theta_0 = [w_1, w_2, w_3, w_4, 0.1, 0.01]^T$, where

$$\begin{aligned} w_1 &\sim U(0, 1), & w_2 &\sim U(0, 4), \\ w_3 &\sim U(4, 12), & w_4 &\sim U(0.02, 0.18), \end{aligned}$$

and the proposed method has been initialised using the distributions from the VI filter ran using θ_0 .

The results of 100 random initialisations using the same data set is summarised in Table 1. The results show that effective parameter estimates have been obtained. For each trial, the proposed method ran until convergence using a dense Hessian approximation (see supplementary material for detail), this required a median of 62 and a maximum of 187 iterations.

Table 1 includes the results of these trials where the third column is the mean estimated value over all trials showing that the identification process has been effective. The almost zero standard deviation (SD) shown in the fourth column is the key point of this test and shows that despite the varying initial estimates, all trials converge to the same point. Therefore, at least on this particular system, the proposed identification method is suitably robust w.r.t. the initially selected parameters and state distributions.

Table 1: Scalar nonlinear identification results

Parameter	True	Sample mean	Sample SD
a	0.5	0.4874	2.1933×10^{-8}
b	2	1.6615	9.3146×10^{-7}
c	8	6.6405	3.4416×10^{-6}
d	0.05	0.0709	7.3018×10^{-8}
q	0	3.0267×10^{-4}	3.8909×10^{-9}
r	0.01	0.0061	2.7087×10^{-9}

For comparison, the URTSS based EM has also been implemented. This approach was selected as it employs similar assumptions to those of the proposed method; namely, Gaussian state distribution, additive Gaussian noise, and the use of the unscented transform to approximate integrals. As this particular model has a linear in parameters structure the maximisation step has been performed using a closed form similar to the expressions given by [Kokkala et al. \(2015\)](#).

As with the linear case, the URTSS EM approach was found to have a very slow rate of convergence. In an attempt to fairly compare against the converged results of the proposed method, which had achieved a significantly lower NLL, the URTSS EM method was allowed to run for 20 000 iterations. As shown in Figure 4a, the URTSS EM did not achieve the performance of the proposed method, which required only 56 iterations. Furthermore, the URTSS EM approach was found to diverge. After the 20 000th iteration, the estimated parameters were given by $\hat{\theta} = [0.527, 3.714, 14.3, 0.01591, 0.01041, 0.009757]^T$ and continued to diverge from the true parameters thereafter.

Whilst the EM framework guarantees a decreasing NLL with each iteration this guarantee is not applicable when approximations are used. Similar divergence of approximate EM has been reported by [Kokkala et al. \(2014\)](#). To investigate which approximation may be responsible, an alternative smoother has been utilised within the EM framework, namely the VI smoother mentioned in Section 3.2. This results in the VI EM identification approach of Section 3.2 and is expected to produce equivalent results to the proposed system identification method albeit with a potentially significantly hampered rate of convergence. To illustrate this, the result of 20 000 VI EM iterations are shown in Figure 4b. The VI EM did not diverge and was found to converge towards the solution obtained using the proposed method. This seems to indicate that, at least for the model under consideration, the divergence of the URTSS EM approach is a result of utilising the URTSS for state estimation and that this divergence may be resolved by utilising the given VI smoother. The runtimes of the proposed method, URTSS EM, and VI EM were 4.36 s, 308.93 s, and 639.42 s respectively.

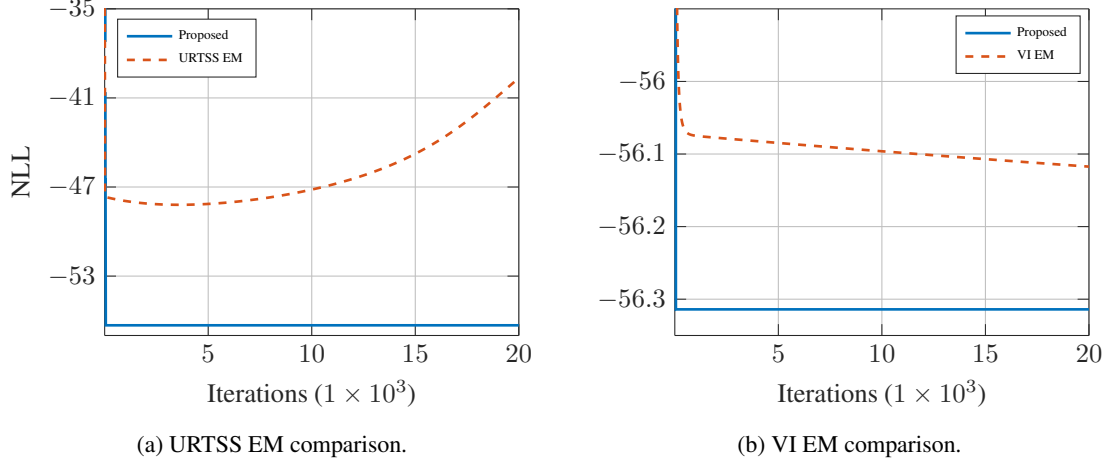


Figure 4: Comparison of NLL obtained when performing system identification for both URTSS EM (Figure 4a) and VI EM (Figure 4b) against the proposed combined method.

4.3 Multidimensional Nonlinear Robot

In this example, we consider the following continuous-time model of a two wheeled robot:

$$\begin{bmatrix} \dot{q}_1(t) \\ \dot{q}_2(t) \\ \dot{q}_3(t) \\ \dot{p}_1(t) \\ \dot{p}_2(t) \end{bmatrix} = \begin{bmatrix} \frac{\cos(q_3(t))p_1(t)}{m} \\ \frac{\sin(q_3(t))p_1(t)}{m} \\ \frac{p_2(t)}{J+ml^2} \\ \frac{-r_1 p_1(t)}{m} - \frac{ml p_2^2(t)}{(J+ml^2)^2} + u_1(t) + u_2(t) \\ \frac{(lp_1(t)-r_2)p_2(t)}{J+ml^2} + au_1(t) - au_2(t) \end{bmatrix}, \quad (28)$$

where $r_1 = 1$, $r_2 = 1$, $a = 0.5$, $m = 5$, $J = 0.2$, $l = 0.15$, $u_1(t)$ is the force applied to the right wheel, $u_2(t)$ is the force applied to the left wheel, and the state vector $x(t) = [q_1(t), q_2(t), q_3(t), p_1(t), p_2(t)]^T$ consists of x-position, y-position, heading, linear momentum, and angular momentum states respectively. The measurement model is given by $y(t) = [q_1(t), q_2(t), q_3(t)]^T$, from which samples corrupted by additive zero mean Gaussian noise are taken at 0.1 s intervals over a 50 second simulation period.

The identification of parameters m , J , l , and additive Gaussian process and measurement noise terms corresponding to a 0.1 s Euler discretisation of the system is considered. Initial parameter estimates are taken to be $\phi = [m, J, l]^T = [10, 4, 0.3]^T$, with the noise terms initialised to $Q = \text{diag}(0.01, 0.01, 0.2^\circ, 0.01, 0.01)$, and $R = \text{diag}(0.1, 0.1, 2^\circ)$.

System identification using URTSS EM, VI EM, and the proposed identification method from Section 3.1.1 using KNITRO (Byrd et al., 2006) with exact first and second derivatives is performed. For both EM methods, 20 000 iterations are used.

For the proposed method, the state distributions have been initialised using the VI filter as per Section 4.2. A subset of estimated parameters using the proposed method are shown in Table 2 and yield adequate estimates of the true parameters despite poor initial values. The parameter estimates were obtained after the 194 iterations required to achieve convergence to a local minima with a final optimality error of 1.38×10^{-10} . The NLL achieved by each

Table 2: Robot Model Identification Results

Parameter	Initial	Estimated	True
m	10	5.0758	5
J	4	2.2761	2
l	0.3	0.1410	0.15

method plotted as a function of iteration count is shown in Figure 5. The results are consistent with the behaviour seen in Section 4.2; URTSS EM does not converge asymptotically, whilst VI EM asymptotically approaches the proposed method. For this example the proposed method required 292.08 s to complete whilst URTSS EM and VI EM required 1.64 h and 7.52 h respectively.

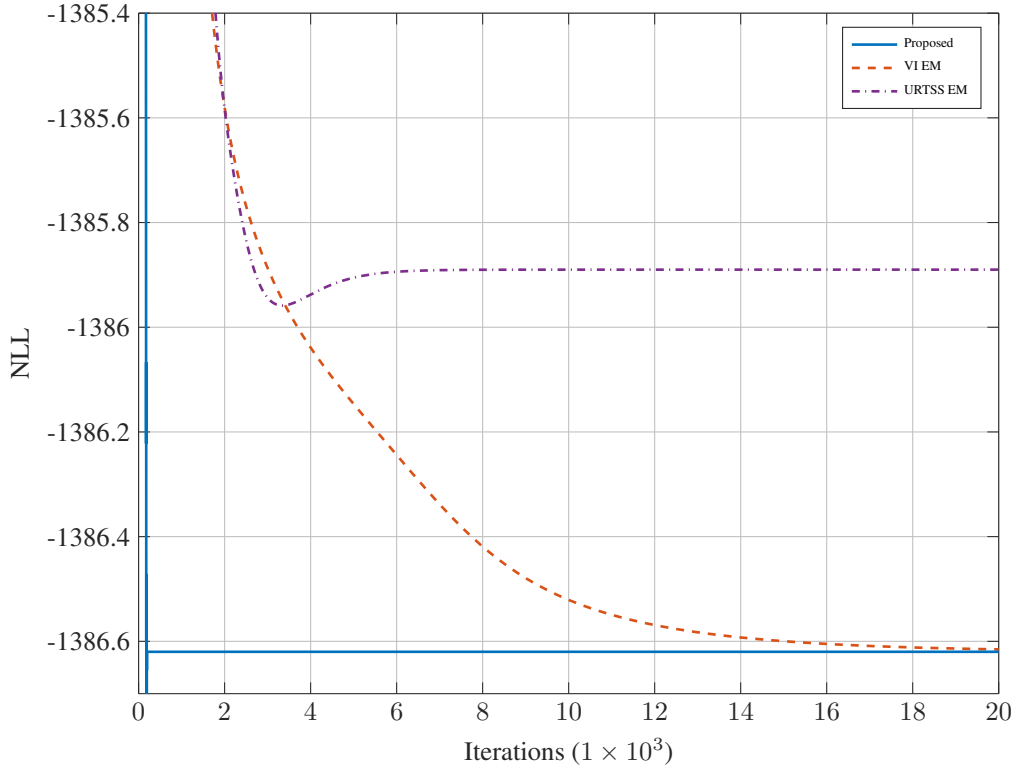


Figure 5: NLL vs. iteration count for each identification method. The line for the proposed method has been extended beyond 194 iterations for clarity.

4.4 Stochastic Volatility Model for Bitcoin price

In this example, we consider estimation of the parameters $\theta = [a, b, c]$ for the following stochastic volatility model:

$$x_{k+1} = a + bx_k + cw_k, \quad (29a)$$

$$y_k = \sqrt{e^{x_k}} v_k, \quad (29b)$$

where $w_k \sim \mathcal{N}(0, 1)$ and $v_k \sim \mathcal{N}(0, 1)$. The data consists of daily Bitcoin price data from November 7, 2015 to November 7, 2017 resulting in 726 measurements. We compare against CPF-SAEM which is a state-of-the-art approach to problems of this general nonlinear structure (Kantas et al., 2015).

For our proposed method, each joint state distribution is initialised with a mean of $[2, 2]^T$ and a diagonal covariance with standard deviations of 0.1. An initial parameter estimate of $\theta = [0, 0.5, 1]^T$ is used for both approaches, and the particle EM employs 50 particles.

The proposed method converges in 19 iterations. In contrast, particle EM does not have a clear convergence criteria, and a limit of 1000 iterations was imposed. The parameter trajectory of both methods is shown in Figure 6 and highlights that whilst similar estimates are obtained the particle EM based approach requires a significantly larger quantity of iterations and only approaches the parameter values obtained by the proposed method. The runtimes of the proposed method and SAEM were 2.53s and 443.53s respectively.

The robustness to initial estimates of the proposed method has also been examined using 100 random initial parameter estimates sampled from $a \sim U(-0.5, 0.5)$, $b \sim U(0, 1.5)$ and $c \sim U(0.25, 2)$. The parameter trajectories for each run are plotted in Figure 7 and show that each initialisation converges to the same parameter estimate.

The robustness to different realisations of the data has also been examined using 100 simulated data sets. For this experiment it is not expected that each run converges to the same value, nor that it converges to the true value, rather the desired result is that the parameter estimates are clustered near the true parameter values. This desired behaviour is shown in Figure 8.

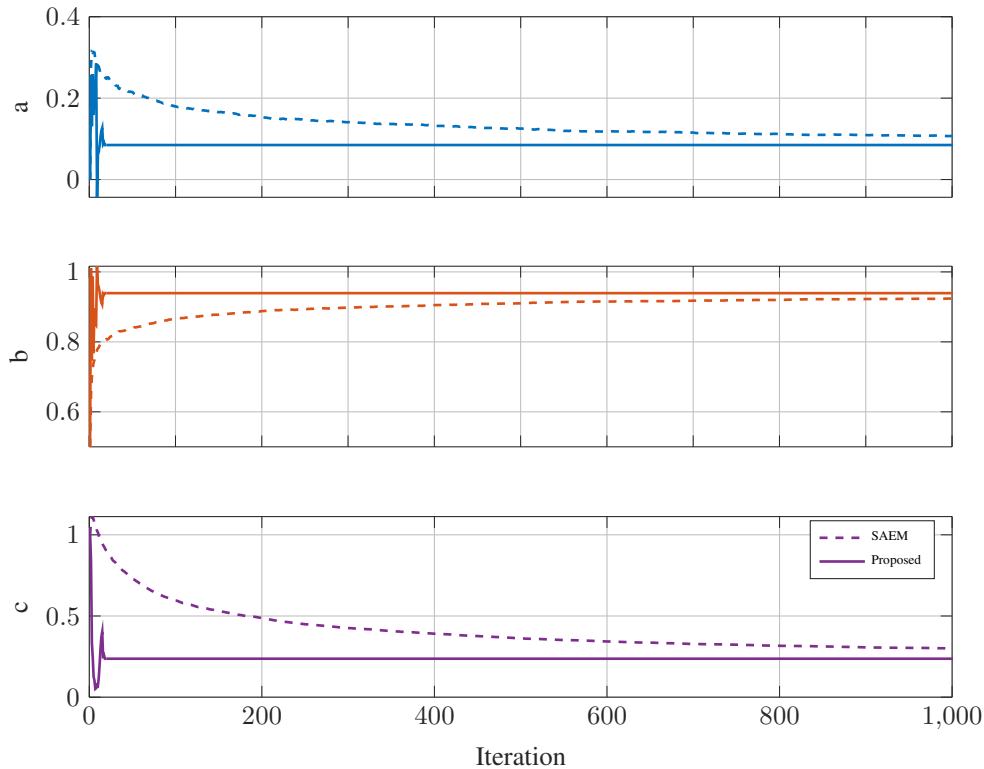


Figure 6: Parameter trajectory vs. iteration count. The lines for the proposed method have been extended beyond 19 iterations for clarity.

5 Related Work

As problem (2) has received enormous attention and remains an active area of research it is impractical to summarise all contributions and related works. Here we present a selection of related works that utilise both VI and EM methods.

Stochastic Differential Equations: The use of variational inference to estimate parameters of continuous-time nonlinear dynamical systems has been considered by [Vrettas et al. \(2011, 2015\)](#) in the context of Stochastic Differential Equations (SDEs). Whilst using some similar high level ideas to our paper in regards to performing state smoothing they possess restrictions on both the structure and values of the noise terms present in the system which results in issues to the parameter estimation process. Also note that the approach applied by [Vrettas et al. \(2011\)](#) is suited only to SDEs and is inapplicable to the discrete state space models we have considered.

General Variational-Interference Approaches: There exist a large amount of work regarding both variational-inference and state space systems. An example of this includes [Archer et al. \(2015\)](#), which considers neural network based state inference, but does not address the parameter estimation problem. Other works such as [Krishnan et al. \(2017\)](#) additionally rely upon assuming all covariance matrices have a strictly diagonal structure. More related works include those of [Maddison et al. \(2017\)](#); [Le et al. \(2018\)](#) and [Naesseth et al. \(2018\)](#), which all consider SMC based methods; however, these works only address the estimation in the context of examining the filtering problem. In [Moretti et al. \(2019\)](#), the use of smoothed distributions within SMC based variational objectives is attempted with the use of neural networks, but this method is incapable of dealing with external inputs signals. Central to all of these works is stochastic gradient descent (SGD) with many of these papers, and indeed the differences between them, being focused on estimation of the gradients, the associated variances and biases, and the impact this has over the overall performance.

Our method is fundamentally different to all of these approaches and shares little in common aside from the use of variational inference to form a lower bound—we have no reliance on mean field assumptions, neural networks, or SGD. Rather, it is an entirely deterministic method utilising exact gradient and Hessian based optimisation

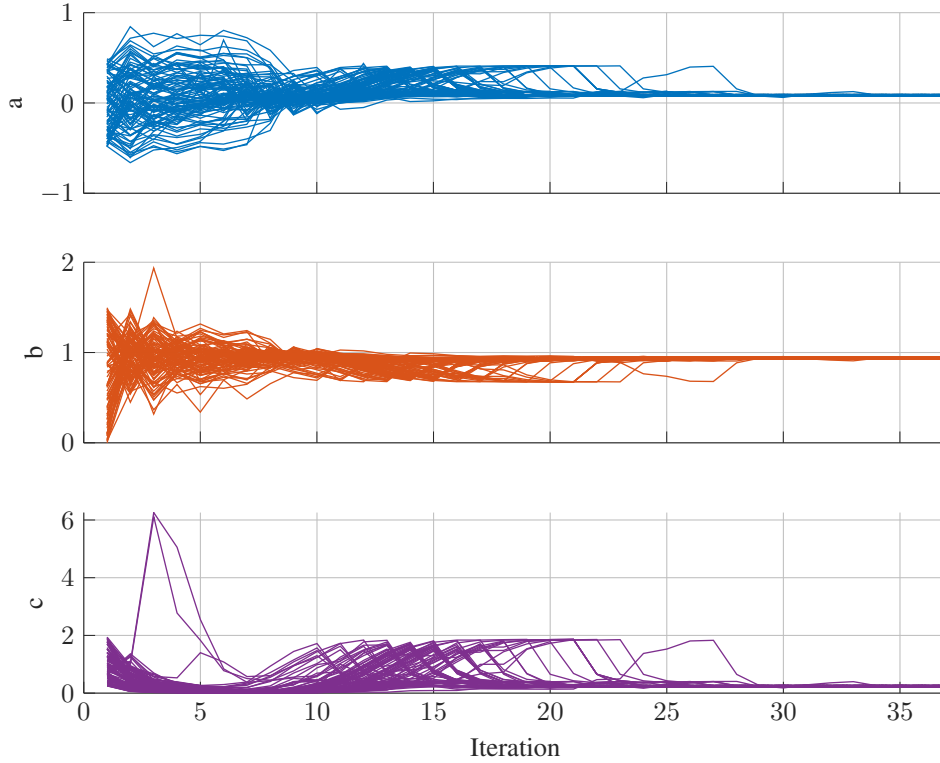


Figure 7: Parameter trajectory vs. iteration count for 100 random initial estimates using the proposed method.

solvers, which enables the simultaneous and efficient estimation of both model parameters and a smoothed state distribution of a user selected structure.

Deterministic Approaches: Despite the popularity of stochastic particle based approaches for nonlinear systems, other deterministic approaches exist. The most related of these are the URTSS EM approaches (Gašperin and Juričić, 2011; Kokkala et al., 2014, 2015; Särkkä, 2013). Whilst not based upon VI, this method is very closely related to our work, with significant assumptions, approximations, and even equations being common with our method. As such, comparisons have been made against this approach.

6 Conclusion

In this paper, we have proposed a variational distribution tailored to nonlinear state-space systems and presented the use of this construction to jointly, and deterministically, estimate state distributions and model parameters. Using the proposed approach, we have additionally provided a clear link between variational inference and EM based parameter estimation approaches. Following this, we have presented extensive numerical experiments using both real and simulated data which demonstrate the efficacy and robustness of our approach.

Future research directions include the development of specialised optimisation algorithms to exploit the structure of the resulting optimisation problems in this paper.

References

- Ala-Luhtala, J., Särkkä, S., Piché, R., Jun. 2015. Gaussian filtering and variational approximations for Bayesian smoothing in continuous-discrete stochastic dynamic systems. *Signal Processing* 111, 124–136.
- Archer, E., Park, I. M., Buesing, L., Cunningham, J., Paninski, L., 2015. Black box variational inference for state space models.
- Byrd, R. H., Nocedal, J., Waltz, R. A., 2006. *Knitro: An Integrated Package for Nonlinear Optimization*. In: *Nonconvex Optimization and Its Applications*. Springer US, pp. 35–59.

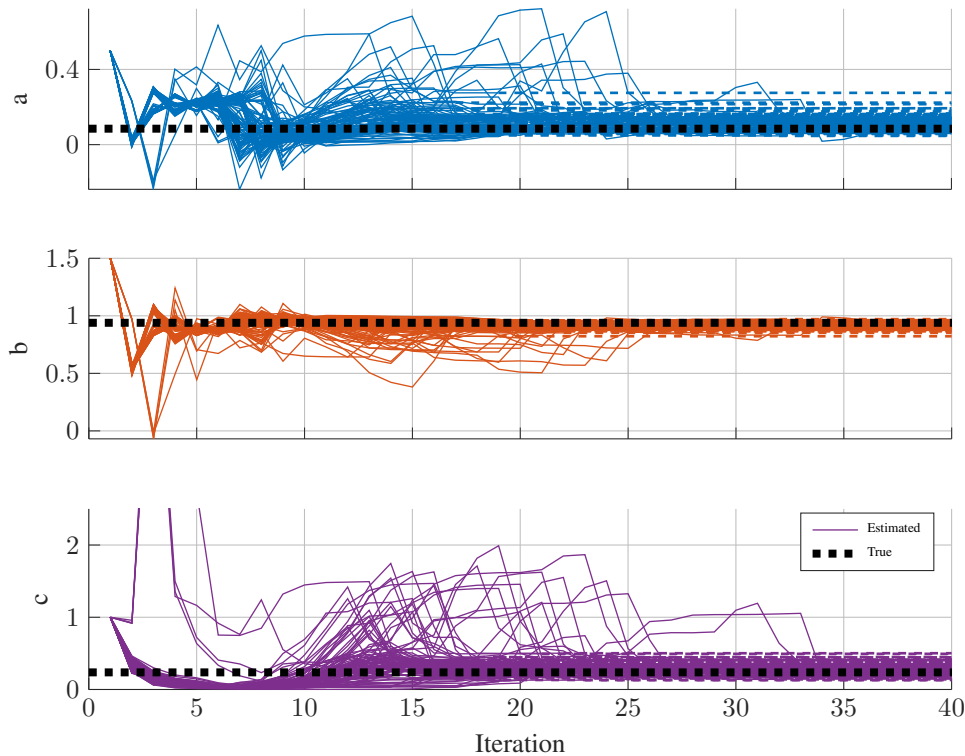


Figure 8: These plots show that performing identification on each of the 100 simulated data-set has resulted in a parameter estimates close to the true values.

- Chitrakleha, S. B., Prakash, J., Raghavan, H., Gopaluni, R. B., Shah, S. L., 2009. Comparison of Expectation-Maximization based parameter estimation using Particle Filter, Unscented and Extended Kalman Filtering techniques. *IFAC Proceedings Volumes* 42 (10), 804–809.
- Darling, J. E., DeMars, K. J., Jul. 2017. Minimization of the Kullback–Leibler Divergence for Nonlinear Estimation. *Journal of Guidance, Control, and Dynamics* 40 (7), 1739–1748.
- Dempster, A. P., Laird, N. M., Rubin, D. B., 1977. Maximum likelihood from incomplete data via the EM algorithm. *JOURNAL OF THE ROYAL STATISTICAL SOCIETY, SERIES B* 39 (1), 1–38.
- Fisher, R., 1922. On the mathematical foundations of theoretical statistics. *Philosophical Transactions of the Royal Society, London, Series A* 222, 309–368.
- Garcia-Fernandez, A. F., Svensson, L., Sarkka, S., Apr. 2017. Iterated Posterior Linearization Smoother. *IEEE Transactions on Automatic Control* 62 (4), 2056–2063.
- Gašperin, M., Juričić, D., Jan. 2011. Application of Unscented Transformation in Nonlinear System Identification. *IFAC Proceedings Volumes* 44 (1), 4428–4433.
- Gibson, S., Ninness, B., Oct. 2005. Robust maximum-likelihood estimation of multivariable dynamic systems. *Automatica* 41 (10), 1667–1682.
- Gordon, N. J., Salmond, D. J., Smith, A. F. M., 1993. Novel approach to nonlinear/non-Gaussian Bayesian state estimation. In: *IEE Proceedings on Radar and Signal Processing*. Vol. 140. pp. 107–113.
- Gultekin, S., Paisley, J., Dec. 2017. Nonlinear Kalman Filtering With Divergence Minimization. *IEEE Transactions on Signal Processing* 65 (23), 6319–6331.
- Jazwinski, A. H., 1970. *Stochastic processes and filtering theory*. Mathematics in science and engineering. New York, USA.
- Jordan, M. I., Ghahramani, Z., Jaakkola, T. S., Saul, L. K., 1999. An introduction to variational methods for graphical models. *Machine learning* 37 (2), 183–233.
- Kantas, N., Doucet, A., Singh, S. S., Maciejowski, J. M., Chopin, N., 2015. On particle methods for parameter estimation in state-space models. *Statistical Science* 30 (3), 328–351.

- Kitagawa, G., 1993. A Monte Carlo filtering and smoothing method for non-Gaussian nonlinear state space models. In: Proceedings of the 2nd US-Japan joint Seminar on Statistical Time Series Analysis. pp. 110–131.
- Kokkala, J., Solin, A., Särkkä, S., Jul. 2014. Expectation Maximization Based Parameter Estimation by Sigma-Point and Particle Smoothing. In: 17th International Conference on Information Fusion (FUSION).
- Kokkala, J., Solin, A., Särkkä, S., 2015. Sigma-Point Filtering and Smoothing Based Parameter Estimation in Nonlinear Dynamic Systems. *Journal of Advances in Information Fusion*.
- Krishnan, R. G., Shalit, U., Sontag, D., 2017. Structured Inference Networks for Nonlinear State Space Models. In: Proceedings of the Thirty-First AAAI Conference on Artificial Intelligence. AAAI'17. AAAI Press, p. 2101–2109.
- Le, T. A., Igl, M., Rainforth, T., Jin, T., Wood, F., 2018. Auto-Encoding Sequential Monte Carlo. In: International Conference on Learning Representations.
- Lindsten, F., may 2013. An efficient stochastic approximation EM algorithm using conditional particle filters. In: 2013 IEEE International Conference on Acoustics, Speech and Signal Processing. IEEE.
- Ljung, L., 1999. *System Identification: Theory for the User*, (2nd edition). Prentice-Hall, Inc., New Jersey.
- Ljung, L., 2008. Perspectives on System Identification. *IFAC Proceedings Volumes* 41 (2), 7172–7184.
- Maddison, C. J., Lawson, J., Tucker, G., Heess, N., Norouzi, M., Mnih, A., Doucet, A., Teh, Y., 2017. Filtering Variational Objectives. In: Guyon, I., Luxburg, U. V., Bengio, S., Wallach, H., Fergus, R., Vishwanathan, S., Garnett, R. (Eds.), *Advances in Neural Information Processing Systems* 30. Curran Associates, Inc., pp. 6573–6583.
- MATLAB, 2018. Optimization Toolbox Release 2018b. The MathWorks, Inc., Natick, Massachusetts, United States.
URL <https://mathworks.com/help/optim/>
- Moretti, A. K., Wang, Z., Wu, L., Pe'er, I., 2019. Smoothing Nonlinear Variational Objectives with Sequential Monte Carlo. In: *Deep Generative Models for Highly Structured Data*, ICLR 2019 Workshop, New Orleans, Louisiana, United States, May 6, 2019.
- Naesseth, C., Linderman, S., Ranganath, R., Blei, D., 09–11 Apr 2018. Variational Sequential Monte Carlo. In: Storkey, A., Perez-Cruz, F. (Eds.), *Proceedings of the Twenty-First International Conference on Artificial Intelligence and Statistics*. Vol. 84 of *Proceedings of Machine Learning Research*. PMLR, Playa Blanca, Lanzarote, Canary Islands, pp. 968–977.
- Särkkä, S., Apr. 2008. Unscented Rauch–Tung–Striebel Smoother. *IEEE Transactions on Automatic Control* 53 (3), 845–849.
- Särkkä, S., 2013. *Bayesian Filtering and Smoothing*. Institute of Mathematical Statistics Textbooks. Cambridge University Press.
- Schön, T. B., Wills, A., Ninness, B., Jan. 2011. System identification of nonlinear state-space models. *Automatica* 47 (1), 39–49.
- Stewart, L., McCarty, P., 1992. The use of Bayesian belief networks to fuse continuous and discrete information for target recognition and discrete information for target recognition, tracking, and situation assessment. In: *Proceedings of SPIE Signal Processing, Sensor Fusion and Target Recognition*. Vol. 1699. pp. 177–185.
- Sun, R., Giles, C. L., 2001. Sequence learning: From recognition and prediction to sequential decision making. *IEEE Intelligent Systems* 16 (4), 67–70.
- Vrettas, M. D., Cornford, D., Opper, M., nov 2011. Estimating parameters in stochastic systems: A variational Bayesian approach. *Physica D: Nonlinear Phenomena* 240 (23), 1877–1900.
- Vrettas, M. D., Opper, M., Cornford, D., jan 2015. Variational mean-field algorithm for efficient inference in large systems of stochastic differential equations. *Physical Review E* 91 (1).
- Vrettas, M. D., Shen, Y., Cornford, D., Mar. 2008. Derivations of Variational Gaussian Process Approximation Framework. Tech. rep., Aston University.

A Numerical Details

In this section we provide details regarding the numerical implementation. Whilst this is detailed in the context of additive Gaussian noise formulation note that the same square root form for the state distributions is utilised for the more general model structure and is hence not detailed elsewhere.

Recall that the optimisation problem we are primarily concerned with is

$$\theta^*, \beta^* = \arg \max_{\theta, \beta} \hat{\mathcal{L}}(\theta, \beta), \quad \text{s.t.} \quad (31). \quad (30)$$

where

$$\mu_k = \eta_k, \quad P_k = \Sigma_k, \quad \begin{bmatrix} P_k & M_k \\ M_k^T & \Sigma_{k+1} \end{bmatrix} \succ 0, \quad \forall k. \quad (31)$$

The purpose of this section is to detail how (30) can be implemented. First an equivalent re-parametrisation of the parametric distribution will be examined, this will be followed by details on robustly calculating $\hat{\mathcal{L}}(\theta, \beta)$, its gradient, and Hessian calculations required for efficient optimisation. Possible methods to initialise all variables are then considered.

It is first noted that to calculate sigma-points the Cholesky decomposition's of all pairwise joints and marginal distributions are required. To simplify all calculations, especially derivative calculations, the Cholesky decomposition's themselves are now to be used to equivalently re-parameterise the normal distributions. Specifically, given S_i such that

$$S_i^T S_i = \begin{bmatrix} P_i & M_i \\ M_i^T & \Sigma_{i+1} \end{bmatrix}, \quad (32)$$

where

$$S_i = \begin{bmatrix} A_i & B_i \\ 0 & C_i \end{bmatrix}, \quad (33)$$

and A_i, C_i are upper triangular. β is now re-parameterised as $\beta \triangleq \{\beta_0, \dots, \beta_T\}$ where

$$\beta_i = \{\mu_i, \eta_{i+1}, A_i, B_i, C_i\}, \quad (34a)$$

$$\beta_T = \{\mu_T, A_T\}. \quad (34b)$$

for $i = 0, \dots, T - 1$. Using this parametrisation the constraints given by (31) are now represented as

$$\text{vech}(B_i^T B_i + C_i^T C_i) = \text{vech}(A_{i+1}^T A_{i+1}), \quad (35)$$

where the vech operator can be used due to the symmetric form. This parametrisation also provides the required Cholesky decomposition's of each marginal distribution as $A_i^T A_i = P_i$. Importantly this results in all sigma-points being linear combinations of the of the variables to be optimised and significantly simplifies derivative calculations. The definiteness constraints in (31), can also be removed as they are satisfied by construction.

To further structure the optimisation process independent copies of the parameter vector ϕ are considered for each time-step, this gives $\vartheta \triangleq \{\phi_0, \dots, \phi_T\}$ where each ϕ_i is used at the corresponding timestep. To stay equivalent to (30) the constraints

$$\phi_{i+1} = \phi_i \quad (36)$$

for $i = 0, \dots, T - 1$ are required. The vector of variables to be passed to a optimisation tool is formed by interleaving, to aid Hessian sparsity, β and ϑ as

$$\psi = [\text{vec}(\beta_0), \phi_0, \dots, \text{vec}(\beta_T), \phi_T], \quad (37)$$

where $\text{vec}(\beta_i)$ denotes vectorising all non structurally zero elements of β_i .

An equivalent problem to (30) is now explicitly given by

$$\psi^* = \arg \max_{\psi} I_1 + I_2^{\text{ID}} + I_3^{\text{ID}} - I_4 \quad (38a)$$

subject to

$$\mu_i = \eta_i \quad (38b)$$

$$\text{vech} (B_i^T B_i + C_i^T C_i) = \text{vech} (A_{i+1}^T A_{i+1}) \quad (38c)$$

$$\phi_{i+1} = \phi_i \quad (38d)$$

for $i = 0, \dots, T - 1$.

Implementation of this problem now requires a method to calculate the objective function and derivatives for both the objective and constraint functions, these calculations will now be examined. Using the square-root parametrisation the objective function can be explicitly calculated utilising

$$\begin{aligned} I_1 &= -\frac{n_x}{2} \log 2\pi - \text{tr} \left(\log \Sigma_p^{\frac{1}{2}} \right) - \frac{1}{2} \text{tr} \left(\Sigma_p^{-1} A_0^T A_0 \right) \\ &\quad - \frac{1}{2} \left(\Sigma_p^{-\frac{T}{2}} (\mu_p - \mu_0) \right)^T \left(\Sigma_p^{-\frac{T}{2}} (\mu_p - \mu_0) \right) \\ I_2^{\text{ID}} &= -\frac{T n_x}{2} \log 2\pi - \frac{T n_x}{2} + \frac{T n_x}{2} \log T \\ &\quad - T \text{tr} (\log q) \\ I_3^{\text{ID}} &= -\frac{T n_x}{2} \log 2\pi - \frac{T n_x}{2} + \frac{T n_x}{2} \log T \\ &\quad - T \text{tr} (\log r) \\ I_4 &= -\frac{(T+1)n_x}{2} \log 2\pi - \frac{(T+1)n_x}{2} \\ &\quad - \text{tr} (\log A_0) - \sum_{i=0}^{T-1} \text{tr} (\log C_i) \end{aligned}$$

where

$$q^T q = \bar{x} \bar{x}^T, \quad r^T r = \bar{y} \bar{y}^T,$$

and $q \in \mathbb{R}^{n_x \times n_x}$, $r \in \mathbb{R}^{n_y \times n_y}$ are upper triangular and calculated using QR decomposition's of \bar{x}^T and \bar{y}^T respectively and log is performed element-wise.

To efficiently perform gradient based optimisation it is additionally required to provide the objective gradient, the constant Jacobian, and a Hessian. Firstly it is noted that the required derivatives for I_1 , I_4 , and all the constraints can be readily obtained with the use of matrix derivative properties. As such these terms are not further examined aside from noting that they result in a block sparse Hessian structure.

The gradients and hessian for I_2 , I_3 are more difficult, both of these terms are of the form

$$\log \det \left(e(\psi) e(\psi)^T \right). \quad (40)$$

where, for I_3 , $e(\psi) = \bar{y}$. I_2 is similarly given. The gradient of this expression is given by

$$\frac{\partial \log \det \left(e(\psi) e(\psi)^T \right)}{\partial \psi_i} \quad (41a)$$

$$\begin{aligned} &= \text{tr} \left(\left(e(\psi) e(\psi)^T \right)^{-1} \frac{\partial e(\psi) e(\psi)^T}{\partial \psi_i} \right) \\ &= 2 \text{tr} \left(\left(e(\psi) e(\psi)^T \right)^{-1} \frac{\partial e(\psi)}{\partial \psi_i} e(\psi)^T \right). \end{aligned} \quad (41b)$$

By again differentiating the second derivative is found to be

$$\frac{\partial^2 \log \det \left(e(\psi) e(\psi)^T \right)}{\partial \psi_i^2} \quad (42a)$$

$$\begin{aligned} &= \frac{\partial}{\partial \psi_i} 2 \text{tr} \left(\left(e(\psi) e(\psi)^T \right)^{-1} \frac{\partial e(\psi)}{\partial \psi_i} e(\psi)^T \right) \\ &= 2 \text{tr} (H_1) + 2 \text{tr} (H_2) + 2 \text{tr} (H_3) \end{aligned} \quad (42b)$$

where

$$H_1 = \left(e(\psi) e(\psi)^T \right)^{-1} \frac{\partial e(\psi)}{\partial \psi_i} \frac{\partial e(\psi)^T}{\partial \psi_i} \quad (42c)$$

$$H_2 = \left(e(\psi) e(\psi)^T \right)^{-1} \frac{\partial}{\partial \psi_i} \left(\frac{\partial e(\psi)}{\partial \psi_i} \right) e(\psi)^T \quad (42d)$$

$$H_3 = \frac{\partial}{\partial \psi_i} \left(\left(e(\psi) e(\psi)^T \right)^{-1} \right) \frac{\partial e(\psi)}{\partial \psi_i} e(\psi)^T \quad (42e)$$

The term H_2 will now be neglected to avoid the requirement of second derivatives of the models functions being available. This can be justified by noting this term involves multiplication the error vector and is a similar assumption to the standard nonlinear least square Hessian approximation. By letting

$$e_n(\psi) = r^{-T} e(\psi), \quad (43a)$$

$$\frac{\partial e_n(\psi)}{\partial \psi_i} = r^{-T} \frac{\partial e(\psi)}{\partial \psi_i}. \quad (43b)$$

denote normalised errors and derivatives are respectively a dense Hessian approximation can then be written as

$$H \approx 2 \operatorname{tr}(H_1) + 2 \operatorname{tr}(H_3) \quad (44a)$$

where

$$H_1 = \left(\frac{\partial e_n(\psi)}{\partial \psi_i} \right)^T \frac{\partial e_n(\psi)}{\partial \psi_i} \quad (44b)$$

$$H_3 = - \left(\frac{\partial e_n(\psi)}{\partial \psi_i} (e_n(\psi))^T \right) \left(\frac{\partial e_n(\psi)}{\partial \psi_i} (e_n(\psi))^T \right) \\ - \left(\frac{\partial e_n(\psi)}{\partial \psi_i} (e_n(\psi))^T \right) \left(\frac{\partial e_n(\psi)}{\partial \psi_i} (e_n(\psi))^T \right)^T. \quad (44c)$$

Here it is noted that H_1 has a sparse block diagonal structure and can hence be formed for large data sets. H_3 is however dense and cannot be tractably formed for large data-sets, as such this term may be required to be neglected when forming the Hessian approximation following the same justification used for H_2 . Information from H_3 can still however be used on large data-sets, this is as Hessian-vector products involving H_3 are tractable by utilising a outer product form.

Returning to the calculation of derivatives for I_2 and I_3 the gradients can be calculated exactly utilising

$$\frac{\partial \log \det \left(e(\psi) e(\psi)^T \right)}{\partial \psi} = 2 \frac{\partial e_n(\psi)}{\partial \psi} \operatorname{vec}(e_n(\psi)) \quad (45)$$

whilst the Hessian can be sparsely approximated as

$$\frac{\partial^2 \log \det \left(e(\psi) e(\psi)^T \right)}{\partial \psi^2} \approx 2 \left(\frac{\partial e_n(\psi)}{\partial \psi} \right)^T \frac{\partial e_n(\psi)}{\partial \psi}, \quad (46)$$

where

$$\frac{\partial e_n(\psi)}{\partial \psi} = \frac{\partial \operatorname{vec}(e_n(\psi))}{\partial \operatorname{vec}^T(\psi)} \quad (47)$$

is sparse.

Specific implementation of these equations requires Jacobians of the process and model functions, as these are application dependant they are not detailed further. With the use of (45) and (46) the gradient and approximate Hessian's of I_2 and I_3 are now available. The optimisation problem of (38) required to perform system identification can now be efficiently addressed using standard nonlinear optimisation tools with the use of both first and second derivative information.

In order to implement the proposed identification approach an initial estimate of all variables is required. As common to all nonlinear system identification approaches an estimate of ϕ , which should be 'reasonable' for the

model under consideration, is required. The initial estimate for Q and R required to implement EM can also be used to initialise the state distributions of the proposed method. This can be achieved by first running a smoother, producing an equivalent initialisation as EM, or alternatively the state distributions produced by the filtering pass alone can be utilised. Additionally the state distributions could be directly initialised using application specific knowledge if available, in this case initial estimates of Q and R are not required.

B VI Smoothing

In the situation that θ is assumed known, then maximising $\mathcal{L}(\theta, \beta)$ over β provides a method of ML based assumed density state smoothing, where the optimal parameter values are provided by

$$\beta^* = \arg \max_{\beta} \mathcal{L}(\theta, \beta). \quad (48)$$

This results in a VI based assumed density state smoother which at a high level is conceptually similar to the state estimation approaches in [Ala-Luhtala et al. \(2015\)](#), [Gultekin and Paisley \(2017\)](#), and [Darling and DeMars \(2017\)](#). The resultant VI based smoother offers an alternative to the typical Unscented Rauch-Tung-Striebel smoother (URTSS) ([Särkkä, 2008](#)) approach and its iterative variants such as the Iterated Posterior Linearization Smoother (IPLS) described by [Garcia-Fernandez et al. \(2017\)](#). The VI smoothing approach, however, has several key differences to these alternatives.

Firstly, unlike the URTSS and its variants, the proposed smoother is not based upon approximating the Kalman filter. This is significant as these approaches only allow for *linear* state corrections and smoothing to be performed, even on nonlinear models ([Darling and DeMars, 2017](#)). Contrary to this, the VI smoother shown allows for *nonlinear* smoothing to occur on nonlinear models.

Secondly, the URTSS approach requires that all state distributions, predicted, filtered, and smoothed, are assumed to be Gaussian. The VI smoother however is less restrictive, assuming only that the smoothed distribution is Gaussian. This allows the VI smoother to be validly utilised in a wider range of situations.

Lastly, the URTSS approach performs function approximations about the prediction densities. However, as discussed by [Garcia-Fernandez et al. \(2017\)](#) better function approximations, and hence state estimation, can be performed utilising the smoothed densities. This is an inherent feature of the VI smoother given here as all integral approximations naturally occur about the estimated smoothed distribution.

These differences are illustrated in [Figure 9](#), where a single time-instant is shown for a 1D Bayesian filtering problem for a nonlinear system. The predicted density is far from the true filtered density and bootstrap particle methods, the UKF and iterated UKF (IUKF) solutions all perform quite poorly. Contrary to this the VI-based filtering solution provides a very good match to the true filtered distribution.

Note that the VI smoothing approach discussed here is implicitly contained within our proposed system identification approach. As such when compared to alternative identification methods such as [Gašperin and Juričić \(2011\)](#); [Chitrakha et al. \(2009\)](#) and [Kokkala et al. \(2014\)](#), which all consider sigma point Rauch-Tung-Striebel smoothing based EM, the proposed identification method also possess the key differences discussed above.

C Examples

This section contains additional details regarding the examples section of the paper.

C.1 Comparison with VSMC

It was desired to compare against Variational Sequential Monte Carlo (VSMC) ([Naesseth et al., 2018](#)) VSMC, particularly on the more involved nonlinear multidimensional robot example and the stochastic volatility example utilising real bitcoin price data.

However, it was experimentally found that the computational requirements of VSMC appear to scale approximately quadratically in the quantity of measurement samples. This is shown in [Figure 10](#) which was obtained using

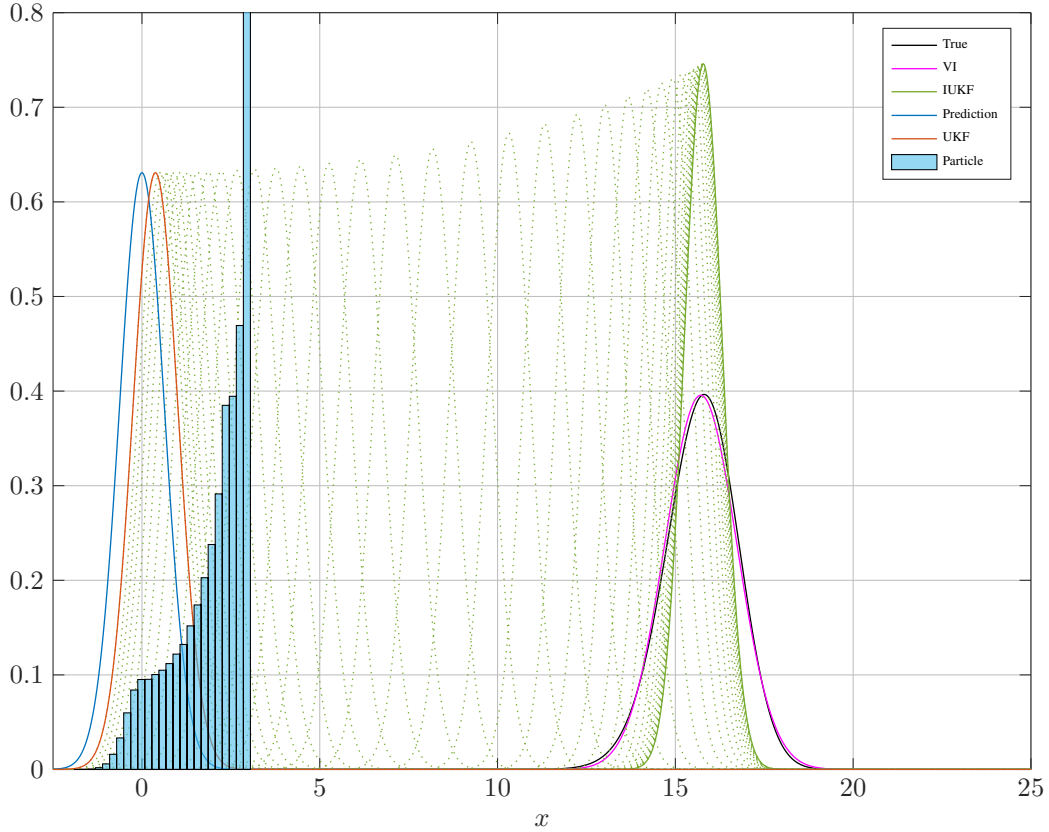


Figure 9: Comparison of differing state estimation approaches for a single timestep. Whilst the IUKF (iterations shown by dotted green) well approximates the true mean only the VI approach has well approximated the true state distribution.

the publicly available code provided from the authors of [Naesseth et al. \(2018\)](#) and only altering the quantity of measurements, T .

This scaling is problematic for the quantity of measurements we have considered in this paper. For example VSMC was found to require approximately 25 seconds per SGD iteration using 4 particles on a scalar linear system with 700 scalar measurements. As all results in [Naesseth et al. \(2018\)](#) seem to require a minimum of 10,000 iterations the run-time required as allow for a comparison with VSMC was deemed prohibitive for the computing infrastructure (laptop) used to obtain all results in this paper.

C.2 Nonlinear Scalar Model

Here we provide additional details regarding the grid based reference solution for this nonlinear system.

In order to effectively evaluate the proposed method Bayes rule has been numerically implemented over a fine grid in order to provide ‘ground truth’ values for the, generally intractable, likelihoods and prediction, filtered, and smoothed state distributions. Based upon prior knowledge of the system and parameter values a grid with a discretisation interval of 2.5×10^{-3} ranging from -25 to 25 has been selected, this results in each joint distribution being represented by a 400 million element two dimensional array. For numerical reasons this grid based approach to Bayes rule has been implemented entirely in log form with extensive use of the log-sum-exp trick. For all grid based results presented each state distribution has been visually examined to ensure all meaningful probability mass is within the grid bounds and that all distributions have enough of a spread such that the discretisation interval is not problematic. The implementation of this grid based method has been successfully checked against the closed form solutions available for suitable linear systems.

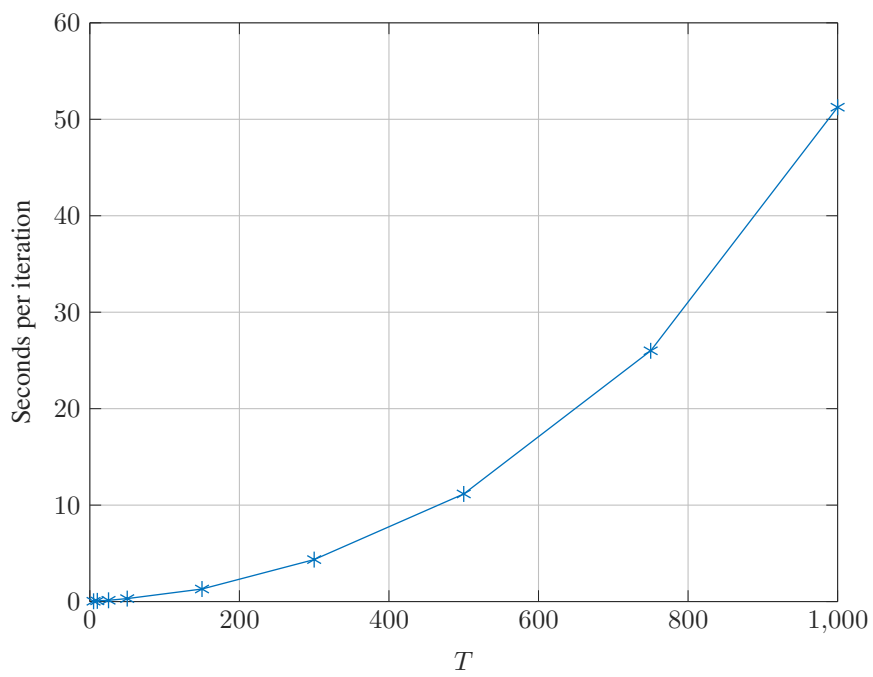


Figure 10: Runtime per iteration using 4 particles on a scalar linear system using VSMC illustrating approximately quadratic scaling with T . Due to the quantity of iterations required for VSMC and the sizes of T we consider this make VSMC computationally prohibitive.